Noise Reduction of JPEG Images by Sampled-Data H^∞ Optimal ε Filters

H. Kakemizu[†,1], M. Nagahara[‡,2], A. Kobayashi[‡,3], Y. Yamamoto[‡,4]

† Texas Instruments ‡ Kyoto University, Kyoto, 606-8501, Japan

1 kakemizu@acs.i.kyoto-u.ac.jp 2 nagahara@i.kyoto-u.ac.jp

3 kobayashi@acs.i.kyoto-u.ac.jp 4 yy@i.kyoto-u.ac.jp

Abstract: We propose a new method to reduce artifacts of digital images decompressed via Joint Photographic Experts Group (JPEG). JPEG images produce blocking and ringing artifacts, which are distinctive especially at low bit rates. We introduce sampled-data H^∞ optimal filters, which reduce such artifacts taking the analog characteristic of the original image into account, combined with ε filters to preserve high frequency details. An example is presented to illustrate the effectiveness of the proposed method.

Keywords: image processing, JPEG, sampled-data H^∞ optimization

1. Introduction

Artifacts in JPEG [9] images are caused mainly by the discrete cosine transform and quantization. In particular, *blocking* and *mosquito* artifacts are well-known characteristics of JPEG images. Blocking artifacts are visible at low bit rates owing to discontinuities between adjacent blocks. On the other hand, mosquitoes are found around edges of decompressed images because of lack of high frequency data.

We treat these artifacts as high frequency noise added to an image before compression, and propose to reduce the noise via sampled-data H^∞ optimization [2]. By sampled-data H^∞ optimization, we optimize the analog performance with an H^∞ optimality criterion. By using that, we can take account of the analog characteristic of the original image (e.g., the 2D frequency distribution of an object to be photographed by a digital camera). Moreover, we combine it with ε filters [3]. They are nonlinear filters which can remove small noise on images and preserve high frequency details. We present an example to show that our method is superior to conventional ones.

2. Design Problem

Consider the block diagram shown in Fig. 1. The in-

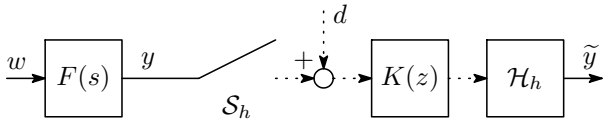

Figure 1: Signal reconstruction

coming signal (image) w first goes through an analog filter $F(s)$ and the filtered signal y becomes nearly (but not entirely) band-limited. The filter $F(s)$ governs the frequency-domain characteristic [1] of the analog signal w. The signal y is then sampled by the sampler $\mathcal{S}_h$ with sampling period h to become a discrete-time (or discrete-space) signal. Then, the signal is corrupted by the additive noise d. The filter $K(z)$ attempts to reduce the noise and to reconstruct the original image. Then the filtered signal becomes an analog (i.e., continuous-time) signal by a hold device $\mathcal{H}_h$ and we obtain the reconstructed signal $\widetilde{y}$.

We thus consider the block diagram shown in Fig. 2 that is the signal reconstruction error system for the

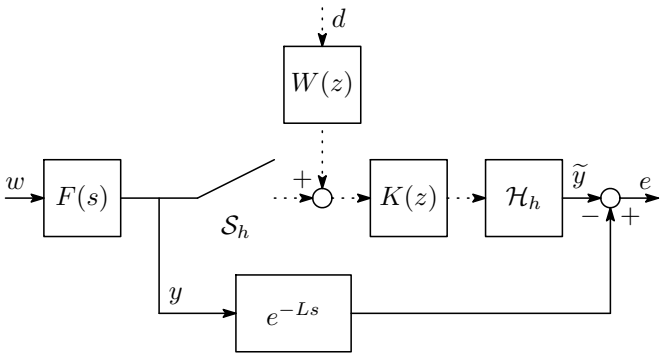

Figure 2: Error system

design. In the diagram the following points are taken into account:

- The time delay e^{-Ls} is introduced because we allow a certain amount of time delay for signal reconstruction.
- The noise obeys a frequency characteristic $W(z)$.

Our design problem is defined as follows:

[1] In the conventional design, $F(s)$ is considered to be an ideal filter that has the cut-off frequency up to the Nyquist frequency

Problem 1 *Given a stable, strictly proper, continuous-time $F(s)$, stable proper discrete-time $W(z)$, sampling period h, find the digital filter $K(z)$ that minimizes*

$$J(K) := \sup_{w\in L^2, d\in \ell^2} \frac{\|e\|_{L^2}^2}{\|w\|_{L^2}^2 + \|d\|_{\ell^2}^2}.$$

3. H^∞ Optimal Filter

Problem 1 involves a continuous-time delay, and hence it is an infinite-dimensional sampled-data H^∞ optimization problem. The problem is, however, reducible to a finite-dimensional discrete-time one via fast sampling/hold approximation [5] or discretization preserving the H^∞ norm [7]. We here discuss the norm preserving discretization.

3.1 Non-causal hold for image reconstruction

By usual, a zero-order hold is used for converting discrete-time signals into continuous-time ones. The most common method is to causally hold the discrete-time signals constant over the sampling intervals as shown in Fig. 3(a). The causal hold is appropriate for causal signals such as audio ones, whereas non-causal hold as shown in Fig. 3(b) is more suitable for non-causal signals such as images. The non-causal hold $\mathcal{H}_h$

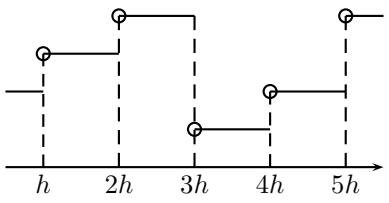

(a) Causal hold

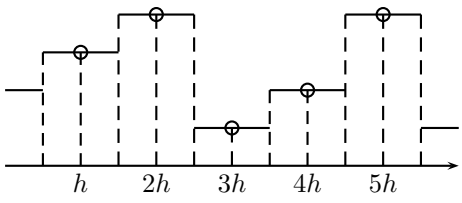

(b) Non-causal hold

Figure 3: Zero-order hold $\mathcal{H}_h$

is given as follows.

$$\begin{aligned} &\mathcal{H}_h : \ell^2 \ni u_d \mapsto u \in L^2, \\ &u(kh+\theta) := u_d[k]\phi(\theta), \\ &\qquad \theta \in [-h/2, h/2), k = 0, 1, 2, \ldots, \end{aligned} \tag{1}$$

where ϕ is a hold function defined by

$$\phi(\theta) := \begin{cases} 1, & \theta \in [-h/2, h/2) \\ 0, & \text{otherwise.} \end{cases}$$

3.2 Reduction to a finite-dimensional problem

Let $\mathcal{T}_{ew}$ denote the input/output operator of the error system shown in Fig. 2, and $\{A, B, C, 0\}$ be a minimal realization of $F(s)$. By the linear fractional transformation [11], $\mathcal{T}_{ew}$ is represented by $\mathcal{F}_\ell(G_0, \mathcal{H}_h K \mathcal{S}_h)$, where

$$G_0(s) := \begin{bmatrix} e^{-Ls}F(s) & -1 \\ F(s) & 0 \end{bmatrix}.$$

Assume $L = mh, m \in \mathbb{Z}_+ := \{0, 1, 2, \ldots\}$. Then, for any $\gamma > 0$, we have [6]

$$\|\mathcal{F}_\ell(G_0, K)\|_\infty < \gamma \Leftrightarrow \|\mathcal{F}_\ell(G, \bar{K})\|_\infty < \gamma,$$

where $\bar{K}(z) := z^m K(z)$ and

$$G(s) := \begin{bmatrix} F(s) & -1 \\ F(s) & 0 \end{bmatrix} = \left[\begin{array}{c|cc} A & B & 0 \\ \hline C & 0 & -1 \\ C & 0 & 0 \end{array}\right].$$

By lifting G, we have the lifted system [2]

$$\breve{G}(z) = \left[\begin{array}{c|cc} \bar{A}_d & \acute{B}_{d1} & \bar{B}_{d2} \\ \hline \grave{C}_{d1} & \breve{D}_{d11} & \grave{D}_{d12} \\ \bar{C}_{d2} & 0 & 0 \end{array}\right], \tag{2}$$

$$\begin{aligned} \bar{A}_d &= \begin{bmatrix} \bar{A} & 0 \\ 0 & 0 \end{bmatrix}, \quad \acute{B}_{d1} = \begin{bmatrix} \acute{B}_1 \\ 0 \end{bmatrix}, \quad \bar{B}_{d2} = \begin{bmatrix} 0 \\ 1 \end{bmatrix}, \\ \grave{C}_{d1} &= \begin{bmatrix} \grave{C}_1 & \grave{C}_{\mathcal{H}} \end{bmatrix}, \quad \bar{C}_{d2} = \begin{bmatrix} C & 0 \end{bmatrix}, \\ \breve{D}_{d11} &= \breve{D}_{11}, \quad \grave{D}_{d12} = \grave{D}_{\mathcal{H}}, \end{aligned}$$

where $\{\bar{A}, \acute{B}_1, \grave{C}_1, \breve{D}_{11}\}$ is a state-space realization of the lifted system of $F(s)$:

$$\begin{aligned} &\begin{cases} x[k+1] = \bar{A}x[k] + (\acute{B}_1 w)[k], \\ y[k](\theta) = (\grave{C}_1 x[k])(\theta) + (\breve{D}_{11} w)[k](\theta), \end{cases} \\ &\bar{A} := e^{Ah}, \\ &\acute{B}_1 : L^2[0,h) \to \mathbb{R}^n : w \mapsto \int_0^h e^{A(h-\tau)} B w(\tau) d\tau, \\ &\grave{C}_1 : \mathbb{R}^n \to L^2[0,h) : x \to Ce^{A\theta}x, \\ &\breve{D}_{11} : L^2[0,h) \to L^2[0,h), \\ &\qquad : w \mapsto \int_0^\theta Ce^{A(\theta-\tau)} B w(\tau) d\tau, \quad \theta \in [0,h), \end{aligned}$$

and $\{\grave{C}_{\mathcal{H}}, \grave{D}_{\mathcal{H}}\}$ is defined by lifting the non-causal hold $\mathcal{H}_h$ (1):

$$\begin{cases} \sigma[k+1] = u_d[k], \\ \tilde{y}[k](\theta) = (\grave{C}_{\mathcal{H}} \sigma[k])(\theta) + (\grave{D}_{\mathcal{H}} u_d[k])(\theta), \end{cases}$$

$$\grave{C}_{\mathcal{H}} : \mathbb{R} \to L^2[0,h), \quad : \sigma \mapsto \phi(\theta + h)\sigma$$
$$\grave{D}_{\mathcal{H}} : \mathbb{R} \to L^2[0,h), \quad : u_d \mapsto \phi(\theta)u_d, \quad \theta \in [0,h).$$

For the sampled-data system $\mathcal{F}_\ell(G, \bar{K})$, a norm-equivalent discrete-time system is obtained [1] assuming $\gamma_h := \|\breve{D}_{11}\| < \gamma$. However, since $\bar{K}$ can be a non-causal filter, it is possible that the optimal γ can be less than $\|\breve{D}_{11}\|$ by a non-causal $\bar{K}$. Therefore, we adopt a discretization method which is independent of controller causality constraints [7].

Let $\breve{\Pi}_B$ be the orthogonal projection of $L^2[0,h)$ on the null space $\mathcal{N}(\acute{B}_{d1})$. This is obtained by $\breve{\Pi}_B = I - \acute{B}_{d1}^*(\acute{B}_{d1}\acute{B}_{d1}^*)^\dagger \acute{B}_{d1}$ where "†" indicates the pseudoinverse. For the system (2), define a discrete-time system $\bar{G}$ by

$$\bar{G}(z) := \left[\begin{array}{c|cc} \bar{A} & \bar{B}_1 & \bar{B}_2 \\ \hline \bar{C}_1 & \bar{D}_{11} & \bar{D}_{12} \\ \bar{C}_2 & 0 & 0 \end{array}\right],$$

where $\bar{B}_1$ is a matrix which satisfies

$$\bar{B}_1\bar{B}_1' = \acute{B}_{d1}\acute{B}_{d1}^*,$$

and $\bar{C}_1$, $\bar{D}_{11}$, $\bar{D}_{12}$ are matrices which satisfy

$$\bar{D}_{11} = \bar{D}_a\bar{B}_1,$$
$$\begin{bmatrix} \bar{C}_1' \\ \bar{D}_a' \\ \bar{D}_{12}' \end{bmatrix}\begin{bmatrix} \bar{C}_1' \\ \bar{D}_a' \\ \bar{D}_{12}' \end{bmatrix}' = \grave{O}_z^*\left(I - \gamma^{-2}\breve{D}_{d11}\breve{\Pi}_B\breve{D}_{d11}^*\right)^{-1}\grave{O}_z,$$
$$\grave{O}_z := \begin{bmatrix}\grave{C}_{d1} & \breve{D}_{d11}\acute{B}_{d1}^*(\acute{B}_{d1}\acute{B}_{d1}^*)^\dagger & \grave{D}_{d12}\end{bmatrix},$$

for $\gamma > \hat{\gamma}_h := \|\breve{D}_{11}\breve{\Pi}_B\|$. Then we have the following theorem.

Theorem 1 *For any stable $\bar{K}$, $\|\mathcal{F}_\ell(\breve{G}, \bar{K})\|_\infty \geq \hat{\gamma}_h$. Moreover, for any stable $\bar{K}$ and any $\gamma > \hat{\gamma}_h$, the followings are equivalent.*

1. $\|\mathcal{F}_\ell(\breve{G}, \bar{K})\|_\infty < \gamma$.
2. $\|\mathcal{F}_\ell(\bar{G}, \bar{K})\|_\infty < \gamma$.

The proof is given by [4]. By using this theorem, we can design the optimal filter $\bar{K}$ as follows.

1. Give $\gamma > \hat{\gamma}_h$ and compute the state-space realization of the discrete-time system $\bar{G}$.
2. Define
$$\bar{G}_{\text{aug}} := \begin{bmatrix} z^{-m}\bar{G}_{11} & \bar{G}_{12} \\ \bar{G}_{21} & 0 \end{bmatrix}$$
where $\bar{G}_{ij}(z) := \bar{C}_i(zI - \bar{A})^{-1}\bar{B}_j + \bar{D}_{ij}$.
3. Solve a discrete-time H^∞ optimization problem
$$\|\mathcal{F}_\ell(\bar{G}_{\text{aug}}, K)\| < \gamma.$$
Then $\bar{K} = z^m K$ satisfies $\|\mathcal{F}_\ell(\breve{G}, \bar{K})\| < \gamma$.

For giving $\gamma > \hat{\gamma}_h$ and computing $\bar{G}$, the following lemma is available.

Lemma 1 *For $\gamma > 0$, define*

$$\Phi(t) = \begin{bmatrix}\Phi_{11}(t) & \Phi_{12}(t) \\ \Phi_{21}(t) & \Phi_{22}(t)\end{bmatrix} := \exp\left(\begin{bmatrix} A & BB' \\ 0 & -A' \end{bmatrix} t\right), \quad (3)$$

$$\Gamma(t) = \begin{bmatrix}\Gamma_{11}(t) & \Gamma_{12}(t) \\ \Gamma_{21}(t) & \Gamma_{22}(t)\end{bmatrix} := \exp\left(\begin{bmatrix} A & BB' \\ -\gamma^{-2}C'C & -A' \end{bmatrix} t\right). \quad (4)$$

Then $\gamma > \hat{\gamma}_h$ if and only if for any $t \in (0, h]$,

$$\det\left(\Gamma_{12}(t)\right) \neq 0.$$

Moreover, we have

$$\bar{B}_1\bar{B}_1' = \begin{bmatrix}\Phi_{12}(h)\Phi_{22}^{-1}(h) & 0 \\ 0 & 0\end{bmatrix}, \quad (5)$$

$$\begin{bmatrix} \bar{C}_1' \\ \bar{D}_a' \\ \bar{D}_{12}' \end{bmatrix}\begin{bmatrix} \bar{C}_1' \\ \bar{D}_a' \\ \bar{D}_{12}' \end{bmatrix}' = \begin{bmatrix} M_{11} & M_{21}' & M_{13} & M_{41}' \\ M_{21} & M_{22} & M_{23} & M_{24} \\ M_{13}' & M_{23}' & M_{33} & M_{43}' \\ M_{41} & M_{24}' & M_{43} & M_{44} \end{bmatrix},$$

where each matrix M_{ij} is given in the appendix.

4. Edge Preservation by ε Filters

Filters designed by the method proposed above are linear ones. It is, however, difficult for linear filters to distinguish original signals and noise in the same frequency bands. ε filters [3] are designed to remove small noise on signals with sharp discontinuities. They distinguish edges and noise by setting a threshold ε on the amplitude of input signals. Since artifacts produced by JPEG compression is relatively small, we effectively remove the noise by the filter proposed above with the ε filter.

The input/output relation of ε filter is given by

$$y[m] = x[m] - \sum_{n=-N}^{N} k[n] \cdot f(x[m] - x[m-n]),$$

where x and y are input and output signals respectively, and k is the impulse response of a filter which satisfies

$$\sum_{n=-N}^{N} k[n] = 1.$$

The function f is a nonlinear function such that for all $x \in \mathbb{R}$,

$$|f(x)| \leq \varepsilon,$$

where $\varepsilon > 0$ is a given constant. Fig. 4 shows an example of $f(x)$, which is defined by

$$f(x) := \begin{cases} x, & |x| \leq \varepsilon, \\ \epsilon, & |x| > \varepsilon. \end{cases}$$

By this nonlinear function, if the difference between

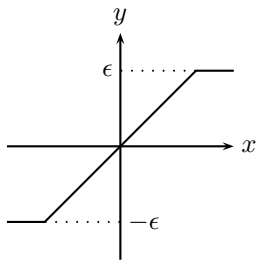

Figure 4: Nonlinear function

samples is small (i.e., $|x[m]-x[m-n]| \le \varepsilon$), the input is just filtered by the filter k, that is,

$$y[k] = x[k] - \sum_{n=-N}^{N} k[n](x[k]-x[k-n]) = \sum_{n=-N}^{N} k[n]x[k-n].$$

On the other hand, if the difference is large (i.e., $|x[m]-x[m-n]| > \varepsilon$), we have

$$|y[m]-x[m]| = \left| \sum_{n=-N}^{N} k[n]\cdot f(x[m]-x[m-n]) \right| \le \epsilon.$$

Consequently, ε filter smooths small-amplitude random signals and keeps large amplitude signal components unchanged. Therefore, without removing sharpness of edges, this filter can suppress small-amplitude random noises.

To make the ε filter suitable for JPEG noise reduction, we adopt the following ε filter.

$$y[m] = \sum_{n=-N_1}^{N_2} k[n]\cdot f_\varepsilon(x[m-n], x[m]), \qquad f_\varepsilon(a,b) := \begin{cases} a, & |a-b| \le \varepsilon, \\ b, & |a-b| > \varepsilon, \end{cases} \tag{6}$$

where the filter coefficients $k[-N_1]$, $k[-N_1+1]$, ..., $k[N_2]$ satisfies

$$|k[0]| \ge |k[n]|, \quad n = -N_1, -N_1+1, \ldots, N_2.$$

Fig. 5 shows this process. Consider the input shown in

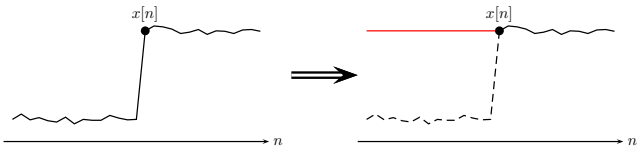

Figure 5: Nonlinear processing by (6)

the left of Fig. 5. If $|x[n]-x[n-l]|$ is larger than ε, we set $x[n-l] := x[n]$ to obtain a signal without edges, as shown in the right of Fig. 5, which is to be filtered by $k[n]$. The threshold level ε can be chosen by the amplitude of noise.

5. Design Example

In this section, we present a design example and compare our method with a conventional one. The design parameters are as follows: the sampling period $h = 1$ and delay step $m = 6$. The analog filter is $F(s) = 1/(Ts+1)^2, T := 10/\pi$. The weighting function for noise is a highpass filter

$$W(z) := 0.02 \cdot \frac{0.2929 - 0.5858z^{-1} + 0.2929z^{-2}}{1 + 0.1716z^{-2}}.$$

The Bode diagram of $W(z)$ is shown in Fig. 6. The

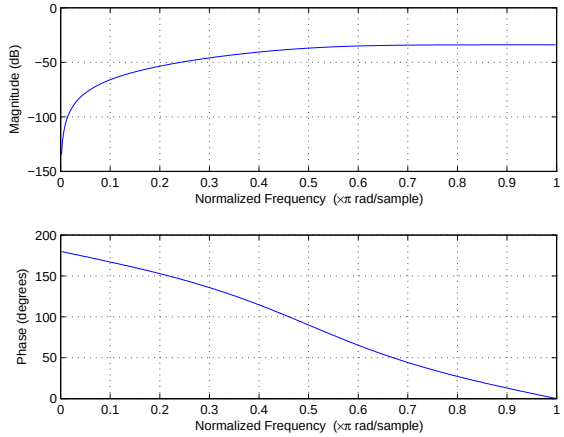

Figure 6: Bode diagram of $W(z)$

threshold level ε is set to be $\varepsilon = 50$.

The impulse response of the proposed filter is shown in Fig. 7. The impulse response is symmetrical about $t = 6$ since the filter is designed with the non-causal hold (1). We process two images shown in Fig. 8(a) and Fig. 8(b). The images are first compressed by JPEG compression, and then processed by the following filters:

1. sampled-data H^∞ optimal filter
2. sampled-data H^∞ optimal ε filter
3. median filter [10]

Table 1 shows SNR (Signal-to-Noise Ratio) of processed images. Since the image "Lena" contains few high frequency components, there is not much difference in SNR (we can see that the proposed filter is the best). However, in the case of the image "Characters" the proposed method is much superior to the others. While median filters have good edge preservation properties, they remove impulses. Therefore, the median filter removes thin lines in characters as shown in Fig. 9(a). On the

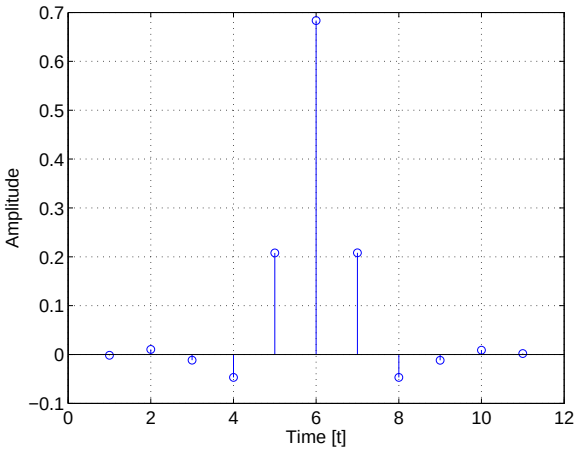

Figure 7: Impulse response of $K(z)$

Table 1: Comparison of SNR [dB]

	Lena	Characters
JPEG Compressed	25.6885	24.6229
H^∞ optimal linear filter	25.7917	19.9852
H^∞ optimal ε filter	26.0136	25.3001
Median filter	25.9288	16.4248

other hand, Fig. 9(b) shows that our method preserves details.

6. Conclusion

We have proposed a new method to reduce blocking and ringing artifacts of JPEG images. We have introduced the sampled-data H^∞ optimal filter, which reduces such artifacts taking the analog characteristic of the original image into account, combined with an ε filter to preserve high frequency details. We have also presented an example to illustrate the effectiveness of the proposed method.

References

[1] B. Bamieh and J. B. Pearson, "A general framework for linear periodic systems with applications to H^∞ sampled-data control," *IEEE Trans. Automat. Contr.*, vol. 37, no. 4, pp. 418–435, 1992.

[2] T. Chen and B. A. Francis, *Optimal Sampled-Data Control Systems*, Springer, 1995.

[3] H. Harashima, K. Odajima, Y. Shishikui and H. Miyakawa, ε-separating nonlinear digital filter and its applications, *IEICE Trans.,* vol. J65-A, no. 4, pp. 297–304, 1982.

(a) Lena

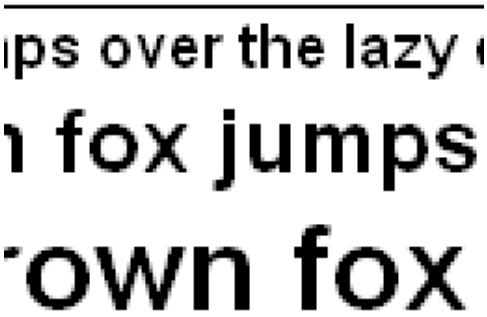

(b) Characters

Figure 8: Original images

[4] H. Kakemizu, *Digital Image Reconstruction via Sampled-Data H^∞ Control Theory*, Master Thesis, Kyoto University, 2005. (in Japanese)

[5] J. P. Keller and B. D. O. Anderson, A new approach to the discretization of continuous-time controllers, *IEEE Trans. Autom. Control*, **AC-37**, pp. 214–223, 1992.

[6] P. P. Khargonekar and Y. Yamamoto, "Delayed signal reconstruction using sampled-data control," in *Proc. 35th IEEE Conf. Decision Control*, Kobe, pp. 1259–1263, 1996.

[7] L. Mirkin and G. Tadmor, Yet another H^∞ discretization, *IEEE Trans. Autom. Control*, **AC-48**, pp. 891–894, 2003.

(a) Median filter

(b) Sampled-data H^∞ optimal ε filter

Figure 9: Filtered images

[8] M. Nagahara and Y. Yamamoto, Design for digital communication systems via sampled-data H^∞ control, *IFAC Workshop on Periodic Control Systems*, pp. 211–216, 2001.

[9] W. Penebaker and J. Mitchell, *JPEG Still Image Compression Standard*, Van Nostrand Reinhold, 1992.

[10] I. Pitas and A. N. Venetsanopoulos, *Nonlinear Digital Filters: Principles and Applications*, Kluwer Academic Publishers, 1990.

[11] K. Zhou, J. Doyle and K. Glover, *Robust and Optimal Control*, Prentice Hall, 1996.

A. Formula for M_{ij}

$$
\begin{aligned}
M_{11} &= \gamma^2 \left\{ \left(I - \Phi_{11}'(h)\Gamma_{22}(h)\right)\Gamma_{12}^{-1}(h) \right. \\
&\quad \left. \times \left(\Phi_{11}(h) - \Gamma_{11}(h)\right) - \Phi_{11}'(h)\Gamma_{21}(h) \right\}, \\
M_{13} &= \gamma^2 \left(I - \Phi_{11}'(h)\Gamma_{22}(h)\right)\Gamma_{12}^{-1}(h), \\
M_{33} &= \gamma^2 \left(\Phi_{22}(h)\Phi_{12}^{-1}(h) - \Gamma_{22}(h)\Gamma_{12}^{-1}(h)\right), \\
M_{21} &= -C\int_0^{h/2} \Gamma_{11}(t)dt \\
&\quad - C\int_0^{h/2} \Gamma_{12}(t)dt \cdot \Gamma_{12}^{-1}(h)\left(\Phi_{11}(h) - \Gamma_{11}(h)\right), \\
M_{22} &= \begin{bmatrix}\gamma^{-2}C & 0\end{bmatrix} \int_0^{h/2} \Gamma(t) \begin{bmatrix} I & 0 \\ \Gamma_{11}(h) & \Gamma_{12}(h)\end{bmatrix}^{-1} \\
&\quad \times \left\{ \begin{bmatrix} I & 0 \\ 0 & 0\end{bmatrix} \int_0^t \Gamma(-s)ds \begin{bmatrix} 0 \\ -C'\end{bmatrix} \right. \\
&\quad \left. - \begin{bmatrix} 0 & 0 \\ I & 0\end{bmatrix} \int_t^{h/2} \Gamma(h-s)ds \begin{bmatrix} 0 \\ -C'\end{bmatrix} \right\} dt + \frac{h}{2} \\
M_{23} &= -C\int_0^h \Gamma_{12}(t)dt \cdot \Gamma_{12}^{-1}(h), \\
M_{24} &= -\begin{bmatrix}\gamma^{-2}C & 0\end{bmatrix} \int_0^{h/2} \Gamma(t)dt \begin{bmatrix} I & 0 \\ \Gamma_{11}(h) & \Gamma_{12}(h)\end{bmatrix}^{-1} \\
&\quad \times \begin{bmatrix} 0 & 0 \\ I & 0\end{bmatrix} \int_{h/2}^h \Gamma(h-s)ds \begin{bmatrix} 0 \\ -C'\end{bmatrix} \\
M_{41} &= -C\int_{h/2}^h \Gamma_{11}(t)dt \\
&\quad - C\int_{h/2}^h \Gamma_{12}(t)dt \cdot \Gamma_{12}^{-1}(h)\left(\Phi_{11}(h) - \Gamma_{11}(h)\right), \\
M_{43} &= -C\int_{h/2}^h \Gamma_{12}(t)dt \cdot \Gamma_{12}^{-1}(h), \\
M_{44} &= \begin{bmatrix}\gamma^{-2}C & 0\end{bmatrix} \int_{h/2}^h \Gamma(t) \begin{bmatrix} I & 0 \\ \Gamma_{11}(h) & \Gamma_{12}(h)\end{bmatrix}^{-1} \\
&\quad \times \left\{ \begin{bmatrix} I & 0 \\ 0 & 0\end{bmatrix} \int_{h/2}^t \Gamma(-s)ds \begin{bmatrix} 0 \\ -C'\end{bmatrix} \right. \\
&\quad \left. - \begin{bmatrix} 0 & 0 \\ I & 0\end{bmatrix} \int_t^h \Gamma(h-s)ds \begin{bmatrix} 0 \\ -C'\end{bmatrix} \right\} dt + \frac{h}{2}
\end{aligned}
$$